Prepared for submission to JHEP

Inadequacy of zero-width approximation for a light Higgs boson signal

Nikolas Kauer[a] **and Giampiero Passarino**[b]

[a] *Department of Physics, Royal Holloway, University of London, Egham TW20 0EX, United Kingdom*
[b] *Dipartimento di Fisica Teorica, Università di Torino, Italy INFN, Sezione di Torino, Italy*

E-mail: n.kauer@rhul.ac.uk, giampiero@to.infn.it

Abstract: In the Higgs search at the LHC, a light Higgs boson ($115\,\text{GeV} \lesssim M_H \lesssim 130\,\text{GeV}$) is not excluded by experimental data. In this mass range, the width of the Standard Model Higgs boson is more than four orders of magnitude smaller than its mass. The zero-width approximation is hence expected to be an excellent approximation. We show that this is not always the case. The inclusion of off-shell contributions is essential to obtain an accurate Higgs signal normalisation at the 1% precision level. For $gg\ (\to H) \to VV$, $V = W, Z$, $\mathcal{O}(10\%)$ corrections occur due to an enhanced Higgs signal in the region $M_{VV} > 2\,M_V$, where also sizable Higgs-continuum interference occurs. We discuss how experimental selection cuts can be used to exclude this region in search channels where the Higgs invariant mass cannot be reconstructed. We note that the $H \to VV$ decay modes in weak boson fusion are similarly affected.

Keywords: Higgs Physics, QCD, Hadron-Hadron Scattering

ArXiv ePrint: 1206.4803

Contents

1 Introduction

A key objective of current particle physics research is the experimental confirmation of a theoretically consistent description of elementary particle masses. In the Standard Model (SM), this is achieved through the Higgs mechanism [1–5], which predicts the existence of one physical Higgs boson. Searches for the SM Higgs boson have been carried out at the Large Electron Positron Collider (LEP) and the Tevatron, which resulted in a lower Higgs mass bound of 114.4 GeV [6], and the exclusion of $M_H \in [147, 180]\,\text{GeV}$ and $M_H \in [100, 103]\,\text{GeV}$ [7], respectively.[1] Higher sensitivity is attainable at the Large Hadron Collider (LHC), which was built as Higgs discovery machine. The combined analysis of the CMS 2011 data of 4.6–4.8 fb^{-1} at 7 TeV excludes $M_H \in [127, 600]\,\text{GeV}$ [8]. Similarly, a recent ATLAS study excludes $M_H \in [111.4, 116.6]\,\text{GeV}$, $M_H \in [119.4, 122.1]\,\text{GeV}$ and $M_H \in [129.2, 541]\,\text{GeV}$ [9]. A light Higgs boson is therefore not excluded by experimental data. In fact, in a seminar on 4th July 2012 at CERN, ATLAS and CMS have presented evidence that a SM-like Higgs boson with $M_H \approx 125$–126 GeV has been observed at the 5σ level. It is therefore important to examine the accuracy of theoretical predictions for Higgs production and decay at the LHC that are used in experimental analyses for light Higgs masses.

For light Higgs masses, the loop-induced gluon-fusion production ($gg \to H$) [10] dominates. Next-to-leading order (NLO) QCD corrections have been calculated in the heavy-top limit [11] as well as with finite t and b mass effects [12–14]. NLO corrections of 80–100% at the LHC motivated the calculation of next-to-next-to-leading order (NNLO) QCD corrections in the heavy-top limit [15–17] enhanced by soft-gluon resummation at next-to-next-to-leading logarithmic (NNLL) level [18, 19] and beyond [20–25]. Fully differential

[1] All bounds and exclusion limits are at 95% C.L.

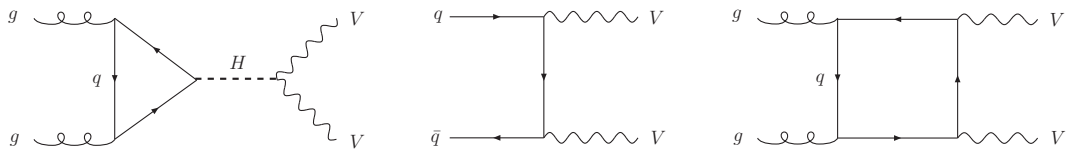

Figure 1. Representative Feynman graphs for the Higgs signal process (left) and the $q\bar{q}$- (center) and gg-initiated (right) continuum background processes at LO.

calculations have been presented in Refs. [26, 27]. The accuracy of the $M_t \to \infty$ approximation at NNLO has been investigated in Refs. [28–33].[2] In addition to higher-order QCD corrections, electroweak (EW) corrections have been computed up to two loops [35–42] and found to be at the 1–5% level. Mixed QCD-EW effects have also been calculated [43]. Refined calculations/updated cross sections for $gg \to H$ have been presented in Refs. [44–48]. Kinematic distributions and NNLO cross sections with experimental selection cuts have also been studied extensively for $gg \to H \to VV \to 4$ leptons ($V = W, Z$) [49, 50] and all other important decay modes (see Ref. [51] and references therein). NLO EW corrections to $H \to VV \to 4$ leptons have been calculated in Refs. [52, 53].

The proper theoretical description of the Higgs boson line shape is an essential ingredient for heavy Higgs searches and has been studied in detail in Ref. [54]. A comparison of the zero-width approximation (ZWA, see below) and finite-width Higgs propagator schemes for inclusive Higgs production and decay can also be found in Refs. [46, 47, 55].[3] In the light Higgs mass range the on-shell width of the SM Higgs boson is more than four orders of magnitude smaller than its mass, for instance 4.03 MeV for a mass of 125 GeV.[4] The ZWA a.k.a. narrow-width approximation, which factorizes the Higgs cross section into on-shell production and on-shell decay when Γ_H approaches zero, is expected to be excellent well below the WW and ZZ thresholds with an error estimate of $\mathcal{O}(\Gamma_H/M_H)$. For Higgs production in gluon fusion, we show in Sections 2 and 3 that this is not always the case. For $gg \to H \to VV$, we find that the deviation between ZWA and off-shell results is particularly large. We therefore take into account the resonance-continuum interference (see Fig. 1, left and right), which was studied in Refs. [60–65] and for related processes in Refs. [66–68]. For studies of the continuum background (see Fig. 1, center and right), we refer the reader to Refs. [69–72] and references therein.

The paper is organised as follows: In Section 2, we briefly review the zero-width approximation and why it can be inadequate. We then present and discuss inclusive results in ZWA and with off-shell effects for the processes $gg \to H \to$ all and $gg \to H \to ZZ$ with $M_H = 125$ GeV including Higgs-continuum interference effects. In Section 3, we extend our ZWA v. off-shell analysis by considering experimental Higgs search procedures, selection criteria and transverse mass observables for all $gg \to H \to VV \to 4$ leptons search channels.

[2] Scale, PDF, strong coupling and heavy-top-limit uncertainties have recently been reappraised in Ref. [34].

[3] The accuracy of the ZWA in the context of beyond-the-SM physics has been studied in Refs. [56–59].

[4] Width computed with HTO, see Section 2.

Higgs-continuum interference effects are again included. Conclusions are given in Section 4.

2 Inclusive analysis

In the SM, the common belief is that for a light Higgs boson the product of on-shell production cross-section (say in gluon-gluon fusion, $gg \to H$) and branching ratios reproduces the correct result to great accuracy. The expectation is based on the well-known result

$$D_H(q^2) = \frac{1}{\left(q^2 - M_H^2\right)^2 + \Gamma_H^2 M_H^2} = \frac{\pi}{M_H \Gamma_H}\,\delta\left(q^2 - M_H^2\right) + PV\left[\frac{1}{\left(q^2 - M_H^2\right)^2}\right] + \sum_{n=0}^{N} c_n(\alpha)\,\delta_n\left(q^2 - M_H^2\right) \tag{2.1}$$

where q^2 is the virtuality of the Higgs boson, M_H and Γ_H are the on-shell Higgs mass and width and PV denotes the principal value (understood as a distribution). Furthermore, $\delta_n(x)$ is connected to the nth derivative of the delta-function by $\delta_n(x) = (-1)^n/n!\,\delta^{(n)}(x)$ and the expansion is in terms of the coupling constant, up to a given order N.

In general, the ZWA can be applied to predict the probability for resonant scattering processes when the total decay width Γ of the resonant particle is much smaller than its mass M. Note that both concepts, on-shell mass and width, are ill-defined for an unstable particle and should be replaced with the complex pole, which is a property of the S-matrix, gauge-parameter independent to all orders of perturbation theory. Nevertheless, let us continue with our qualitative argument: in the limit $\Gamma \to 0$, the mod-squared propagator

$$D(q^2) = \left[\left(q^2 - M^2\right)^2 + (M\Gamma)^2\right]^{-1} \tag{2.2}$$

with 4-momentum q approaches the delta-function limit of Eq. (2.1), i.e.

$$D(q^2) \sim K\,\delta(q^2 - M^2), \qquad K = \frac{\pi}{M\Gamma} = \int_{-\infty}^{+\infty} dq^2\, D(q^2). \tag{2.3}$$

The scattering cross-section σ thus approximately decouples into on-shell production (σ_p) and decay as shown in Eqs. (2.4)–(2.6), where s is the total 4-momentum squared, argument based on the scalar nature of the resonance. Based on the scales occurring in $D(q^2)$, the conventional error estimate is $\mathcal{O}(\Gamma/M)$. This will not be accurate when the q^2 dependence of $|\mathcal{M}_p|^2$ or $|\mathcal{M}_d|^2$ is strong enough to compete with the q^2 dependence of D. An interesting example is $gg \to H \to VV$, where $\sum |\mathcal{M}_d(q^2)|^2 \sim (q^2)^2$ above $2\,M_V$. We note that similar effects have been observed for processes in SM extensions [56–59].

$$\sigma = \frac{1}{2s}\left[\int_{q^2_{\min}}^{q^2_{\max}} \frac{dq^2}{2\pi}\left(\int d\phi_p |\mathcal{M}_p(q^2)|^2 D(q^2) \int d\phi_d |\mathcal{M}_d(q^2)|^2\right)\right] \tag{2.4}$$

$$\sigma_{\text{ZWA}} = \frac{1}{2s}\left(\int d\phi_p |\mathcal{M}_p(M^2)|^2\right)\left(\int_{-\infty}^{\infty} \frac{dq^2}{2\pi} D(q^2)\right)\left(\int d\phi_d |\mathcal{M}_d(M^2)|^2\right) \tag{2.5}$$

$$\sigma_{\text{ZWA}} = \frac{1}{2s}\left(\int d\phi_p |\mathcal{M}_p|^2\right)\frac{1}{2M\Gamma}\left(\int d\phi_d |\mathcal{M}_d|^2\right)\Big|_{q^2=M^2} \tag{2.6}$$

An important observation is that the Breit-Wigner distribution does not drop off nearly as fast as, for instance, a Gaussian. The relative contribution of the tail more than n widths from the peak can be estimated as $1/(n\pi)$, because [73]

$$\int_{(M-n\Gamma)^2}^{(M+n\Gamma)^2} \frac{dq^2}{2\pi} \frac{1}{(q^2-M^2)^2+(M\Gamma)^2} \approx \frac{1}{2M\Gamma}\left(1-\frac{1}{n\pi}\right). \tag{2.7}$$

Since the width of a light Higgs is so small, $n = 1000$ corresponds to only a few GeV, beyond which one would expect less than 0.04% of the signal cross section.

A potential worry, addressed in this paper, is: to which level of accuracy does the ZWA approximate the full off-shell result, given that at $M_H = 125\,\text{GeV}$ the on-shell width (very close to the imaginary part of the complex pole) is 4.03 MeV. When searching for the Higgs boson around 125 GeV one should not care about the region $M_{\text{ZZ}} > 2\,M_Z$ but, due to limited statistics, theory predictions for the normalisation in $\bar{q}q - gg \to ZZ$ are used over the entire spectrum in the ZZ invariant mass.

Therefore, the question is not to dispute that off-shell effects are depressed by a factor Γ_H/M_H, as shown in Eq. (2.1), but to move away from the peak in the invariant mass distribution and look at the behavior of the distribution, no matter how small it is compared to the peak; is it really decreasing with M_{ZZ}? Is there a plateau? For how long is the plateau lasting? How does that affect the total cross-section if no cut is made?

In this section, we consider the signal (S) in the complex-pole scheme (CPS) of Refs. [54, 74, 75]

$$\sigma_{gg\to ZZ}(S) = \sigma_{gg\to H\to ZZ}(M_{\text{ZZ}}) = \frac{1}{\pi}\,\sigma_{gg\to H}\,(M_{\text{ZZ}})\,\frac{M_{\text{ZZ}}^4}{\left|M_{\text{ZZ}}^2 - s_H\right|^2}\,\frac{\Gamma_{H\to ZZ}\,(M_{\text{ZZ}})}{M_{\text{ZZ}}}, \tag{2.8}$$

where s_H is the Higgs complex pole, parametrized by $s_H = \mu_H^2 - i\,\mu_H\,\gamma_H$. Note that γ_H is not the on-shell width, although the numerical difference is tiny for low values of μ_H, as shown in Ref. [54].

The production cross-section, $\sigma_{gg\to H}$, is computed with NNLO QCD corrections (see Ref. [51]) and NLO EW ones [38]. The partial decay width of the off-shell Higgs boson of virtuality M_{ZZ} ($\Gamma_{H\to ZZ}$), is computed at NLO with leading NNLO effects in the limit of large Higgs boson mass, see Ref. [76]. Numerical results in this section are obtained with the program HTO (G. Passarino, unpublished) that allows for the study of the Higgs boson lineshape, in gluon-gluon fusion, using complex poles. Our results refer to $\sqrt{s} = 8\,\text{TeV}$ and are based on the MSTW2008 PDF sets [77]. They are implemented according to the OFFP scheme, see Eq. (45) of Ref. [54]. Furthermore, we set the renormalization and factorization scale to the Higgs virtuality.

Away (but not too far away) from the narrow peak the propagator and the off-shell H width behave like

$$D_H\left(M_{\text{ZZ}}^2\right) \approx \frac{1}{\left(M_{\text{ZZ}}^2 - \mu_H^2\right)^2}, \qquad \frac{\Gamma_{H\to ZZ}\,(M_{\text{Z}})}{M_{\text{ZZ}}} \sim G_{\text{F}}\,M_{\text{ZZ}}^2 \tag{2.9}$$

above threshold with a sharp increase just below it (it increases from $1.62 \cdot 10^{-2}\,\text{GeV}$ at 175 GeV to $1.25 \cdot 10^{-1}\,\text{GeV}$ at 185 GeV). Our result for the VV ($V = W, Z$) invariant

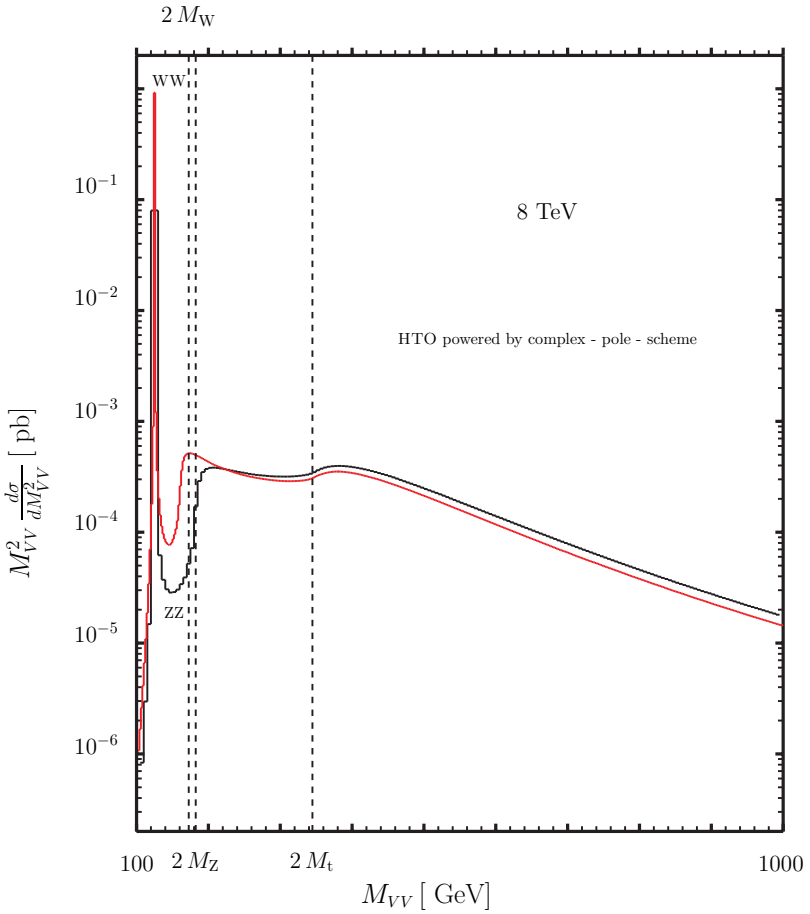

Figure 2. The NNLO ZZ (black) and WW (red) invariant mass distributions in $gg \to VV$ for $\mu_H = 125\,\text{GeV}$.

mass distribution is shown in Fig. 2. It confirms that, above the peak, the distribution is decreasing until the effects of the VV threshold become effective with a visible increase followed by a plateau, by another jump at the $t\bar{t}$-threshold, beyond which the signal distribution decreases almost linearly (on a logarithmic scale). For $gg \to H \to \gamma\gamma$ the effect is drastically reduced and confined to the region $M_{\gamma\gamma}$ between 157 GeV and 168 GeV, where the distribution is already five orders of magnitude below the peak.

What is the net effect on the total cross-section? We show it for ZZ in Table 1 where the contribution above the ZZ-threshold amounts to 7.6%. We have checked that the effect does not depend on the propagator function, complex-pole propagator or Breit-Wigner distribution. The size of the effect is related to the shape of the distribution function. The complex-mass scheme can be translated into a more familiar language by introducing the Bar-scheme [54]. Performing the well-known transformation

$$\overline{M}_H^2 = \mu_H^2 + \gamma_H^2\,, \qquad \mu_H\,\overline{\Gamma}_H = \overline{M}_H\,\gamma_H. \tag{2.10}$$

	Tot[pb]	$M_{\rm ZZ} > 2\,M_Z$[pb]	R[%]
$gg \to H \to$ all	19.146	0.1525	0.8
$gg \to H \to ZZ$	0.5462	0.0416	7.6

Table 1. Total cross-section for the processes $gg \to H \to ZZ$ and $gg \to H \to$ all; the part of the cross-section coming from the region $M_{\rm ZZ} > 2\,M_Z$ is explicitly shown, as well as the ratio.

100–125	125–150	150–175	175–200	200–225	225–250	250–275
0.252	0.252	$0.195 \cdot 10^{-3}$	$0.177 \cdot 10^{-2}$	$0.278 \cdot 10^{-2}$	$0.258 \cdot 10^{-2}$	$0.240 \cdot 10^{-2}$

Table 2. Bin-by-bin integrated cross-section for the process $gg \to H \to ZZ$. The first row gives the bin in GeV, the second row gives the corresponding cross-section in pb.

a remarkable identity follows (defining the so-called Bar-scheme):

$$\frac{1}{M^2_{\rm ZZ} - s_H} = \left(1 + i\,\frac{\overline{\Gamma}_H}{\overline{M}_H}\right)\left(M^2_{\rm ZZ} - \overline{M}^2_H + i\,\frac{\overline{\Gamma}_H}{\overline{M}_H}\,M^2_{\rm ZZ}\right)^{-1}, \tag{2.11}$$

showing that the complex-pole scheme is equivalent to introducing a running width in the propagator with parameters that are not the on-shell ones. Special attention goes to the numerator in Eq. (2.11) which is essential in providing the right asymptotic behavior when $M_{\rm ZZ} \to \infty$, as needed for cancellations with the rest of the amplitude. Therefore, it is not advisable to use a naive, running-width Breit-Wigner distribution or to use a propagator with $M^2_{\rm ZZ} - M^2_H + i\,M_H\,\Gamma_H(M^2_{\rm ZZ})$.

In Table 2, we present the invariant mass distribution integrated bin-by-bin. If we take the ZWA value for the production cross-section at 8 TeV and for $\mu_H = 125\,\text{GeV}$ (19.146 pb) and use the branching ratio into ZZ of $2.67 \cdot 10^{-2}$ we obtain a ZWA result of 0.5203 pb with a 5% difference w.r.t. the off-shell result, fully compatible with the 7.6% effect coming from the high-energy side of the resonance. In Table 1, we also see that the effect is much less evident if we sum over all final states with a net effect of only 0.8%. This agrees well with the deviation of 0.5% between ZWA and fixed-width Breit-Wigner scheme (FWBW) given in Table 1 of Ref. [46] for $M_H = 120\,\text{GeV}$. At $M_H = 125\,\text{GeV}$, de Florian-Grazzini obtain a 0.3%–0.4% deviation between ZWA and CPS (or FWBW) with "pure massless NNLO," i.e. without resummation, heavy quark effects and EW corrections, and a slightly smaller deviation for the full calculation [78]. For $gg \to H \to$ all, one can thus expect deviations of $\mathcal{O}(1\%)$ depending on the particular implementation of the calculation.

Of course, the signal per se is not a physical observable and one should always include background and interference. In Fig. 3 we show the complete LO result for $gg \to ZZ$ calculated with HTO with a cut of $0.25\,M_{\rm ZZ}$ on the transverse momentum of the Z. The large destructive effects of the interference above the resonant peak wash out the peculiar structure of the signal distribution. If one includes the region $M_{\rm ZZ} > 2\,M_Z$ in the analysis then the conclusion is: interference effects are relevant also for the low Higgs mass region, at least for the $ZZ(WW)$ final state. It is worth noting again that the discussed effect on

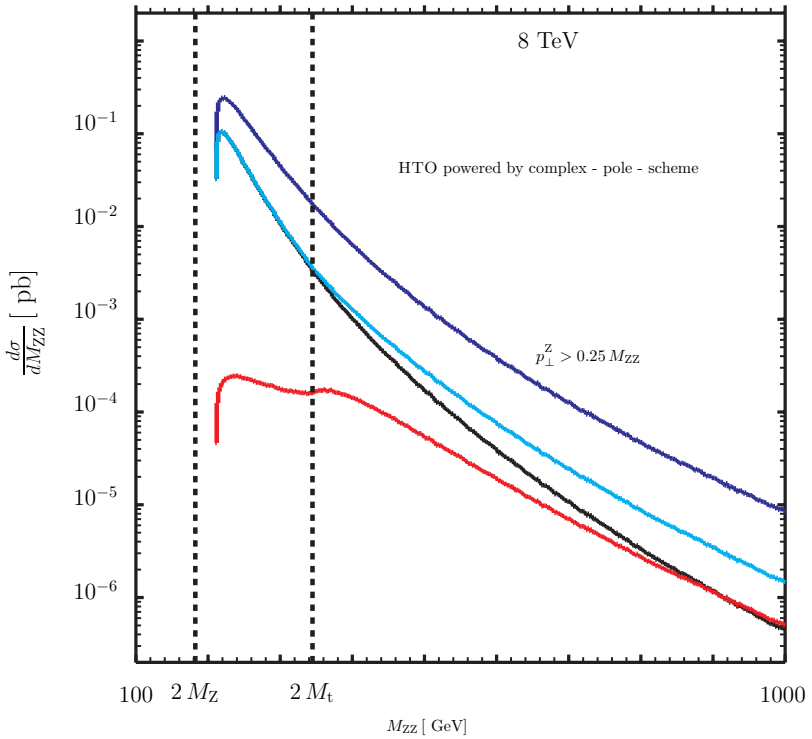

Figure 3. The LO ZZ invariant mass distribution $gg \to ZZ$ for $\mu_H = 125\,\text{GeV}$. The black line is the total, the red line gives the signal while the cyan line gives signal plus background; the blue line includes the $q\bar{q} \to ZZ$ contribution.

the signal has nothing to do with Γ_H/M_H effects; above the ZZ-threshold the distribution is higher than expected (although tiny w.r.t. the narrow peak) and stays roughly constant up to the $t\bar{t}$-threshold after which we observe an almost linear decrease. This is why the total cross-section is affected (in the ZZ final state) at the 5% level.

To conclude our inclusive analysis, we note that our findings are driven by the interplay between the q^2-dependence of the Higgs propagator and the decay matrix element. They should hence not only apply to Higgs production in gluon fusion, but also to Higgs production in weak boson fusion (WBF). The enhancement for $H \to VV$ above M_{VV} may even be stronger in WBF, because $\sigma(q\bar{q} \to q\bar{q}H)$ decreases less rapidly than $\sigma(gg \to H)$ with increasing Higgs invariant mass.[5]

3 Analysis with experimental selection cuts

In this section, we adopt the common selection cuts definition between ATLAS and CMS for $H \to VV$ processes ($V = W, Z$) [81, 82] and calculate parton-level $gg \to H \to VV \to$ leptons cross sections at LO using gg2VV [83] based on Refs. [62, 65, 84–87], with

[5] Preliminary results for inclusive WBF Higgs production reveal effects similar to $gg \to H \to$ all, yielding a deviation of 1% between ZWA and FWBW (but no difference between FWBW and CPS as expected for $M_H = 125\,\text{GeV}$) [79, 80].

Higgs in ZWA as well as off-shell including interference with continuum VV production (where γ^* contributions are also included).[6] All results are given for a single lepton flavour combination. No flavour summation is carried out for charged leptons or neutrinos. As input parameters, we use the specification of the LHC Higgs Cross Section Working Group in App. A of Ref. [45] with NLO Γ_V and G_μ scheme. Finite top and bottom quark mass effects are included. Lepton masses are neglected. We consider the Higgs masses 125 GeV and 200 GeV with $\Gamma_H = 0.004434$ GeV and 1.428 GeV, respectively. The Higgs widths have been calculated with HDECAY [88]. The fixed-width prescription is used for Higgs and weak boson propagators. The renormalisation and factorisation scales are set to $M_H/2$. The PDF set MSTW2008NNLO [77] with 3-loop running for $\alpha_s(\mu^2)$ and $\alpha_s(M_Z^2) = 0.11707$ is used. The CKM matrix is set to the unit matrix, which causes a negligible error [65].

The accuracy of the ZWA Higgs cross section and the impact of off-shell effects is assessed with the ratio

$$R_0 = \frac{\sigma_{H,\mathrm{ZWA}}}{\sigma_{H,\mathrm{offshell}}} \,. \tag{3.1}$$

To facilitate comparison with off-shell M_{VV} distributions, we define the ZWA M_{VV} distribution as suggested by Eq. (2.5):

$$\left(\frac{d\sigma}{dM_{VV}}\right)_{\mathrm{ZWA}} = \sigma_{H,\mathrm{ZWA}} \, \frac{M_H\Gamma_H}{\pi} \, \frac{2M_{VV}}{\left(M_{VV}^2 - M_H^2\right)^2 + (M_H\Gamma_H)^2} \,. \tag{3.2}$$

Each signal process $gg \to H \to VV \to$ leptons (with amplitude $\mathcal{M}_H$) and corresponding continuum background process $gg \to VV \to$ leptons (with amplitude $\mathcal{M}_{\mathrm{cont}}$) have identical initial and final states. Hence interference occurs, and the distinction between signal and background cross sections becomes blurred:

$$|\mathcal{M}_{\mathrm{VV}}|^2 = |\mathcal{M}_H + \mathcal{M}_{\mathrm{cont}}|^2 = |\mathcal{M}_H|^2 + |\mathcal{M}_{\mathrm{cont}}|^2 + 2\,\mathrm{Re}(\mathcal{M}_H\mathcal{M}_{\mathrm{cont}}^*) \,. \tag{3.3}$$

We assess interference effects using a $(S+B)$-inspired interference measure,

$$R_1 = \frac{\sigma(|\mathcal{M}_{\mathrm{VV}}|^2)}{\sigma(|\mathcal{M}_H|^2 + |\mathcal{M}_{\mathrm{cont}}|^2)} \,, \tag{3.4}$$

and a $(S/\sqrt{B})$-inspired measure,

$$R_2 = \frac{\sigma(|\mathcal{M}_H|^2 + 2\,\mathrm{Re}(\mathcal{M}_H\mathcal{M}_{\mathrm{cont}}^*))}{\sigma(|\mathcal{M}_H|^2)} \,. \tag{3.5}$$

In the following, charged leptons are denoted by ℓ.

3.1 $gg \to H \to ZZ \to \ell\bar{\ell}\ell\bar{\ell}$ and $\ell\bar{\ell}\ell'\bar{\ell}'$ at $M_H = 125$ GeV

The same- and different-flavour 4-charged-lepton channels have been analysed by ATLAS [89] and CMS [90] for Higgs masses in the range 110–600 GeV. In these search channels, the invariant mass of the intermediate Higgs ($M_{H^*} \equiv M_{ZZ}$) can be reconstructed. The

[6] All cross sections are evaluated with a $p_T(V) > 1$ GeV cut. This technical cut prevents numerical instabilities when evaluating the continuum amplitude.

	$gg\ (\to H) \to ZZ \to 4\ell$ and $2\ell\,2\ell'$						
	σ [fb], pp, $\sqrt{s} = 8\,\text{TeV}$, $M_H = 125\,\text{GeV}$				ZWA	interference	
mode	H_{ZWA}	H_{offshell}	cont	$\lvert H_{\text{ofs}}+\text{cont}\rvert^2$	R_0	R_1	R_2
$\ell\bar{\ell}\,\ell\bar{\ell}$	0.0748(2)	0.0747(2)	0.000437(3)	0.0747(6)	1.002(3)	0.994(8)	0.994(8)
$\ell\bar{\ell}\,\ell'\bar{\ell}'$	0.1395(2)	0.1393(2)	0.000583(2)	0.1400(3)	1.002(2)	1.001(2)	1.001(2)

Table 3. Cross sections for $gg\ (\to H) \to ZZ \to \ell\bar{\ell}\ell\bar{\ell}$ and $\ell\bar{\ell}\ell'\bar{\ell}'$ in pp collisions at $\sqrt{s} = 8\,\text{TeV}$ for $M_H = 125\,\text{GeV}$ and $\Gamma_H = 0.004434\,\text{GeV}$ calculated at LO with gg2VV. The zero-width approximation (ZWA) and off-shell Higgs cross sections, the continuum cross section and the sum of off-shell Higgs and continuum cross sections including interference are given. The accuracy of the ZWA and the impact of off-shell effects are assessed with $R_0 = \sigma_{H,\text{ZWA}}/\sigma_{H,\text{offshell}}$. Interference effects are illustrated through $R_1 = \sigma(|\mathcal{M}_H + \mathcal{M}_{\text{cont}}|^2)/\sigma(|\mathcal{M}_H|^2 + |\mathcal{M}_{\text{cont}}|^2)$ and $R_2 = \sigma(|\mathcal{M}_H|^2 + 2\,\text{Re}(\mathcal{M}_H\mathcal{M}^*_{\text{cont}}))/\sigma(|\mathcal{M}_H|^2)$. γ^* contributions are included in $\mathcal{M}_{\text{cont}}$. Applied cuts: $|M_{ZZ} - M_H| < 1\,\text{GeV}$, $p_{T\ell} > 5\,\text{GeV}$, $|\eta_\ell| < 2.5$, $\Delta R_{\ell\ell} > 0.1$, $76\,\text{GeV} < M_{\ell\bar{\ell},12} < 106\,\text{GeV}$ and $15\,\text{GeV} < M_{\ell\bar{\ell},34} < 115\,\text{GeV}$ (see main text), $M_{\ell\bar{\ell}} > 4\,\text{GeV}$. Cross sections are given for a single lepton flavour combination. No flavour summation is carried out for charged leptons or neutrinos. The integration error is given in brackets.

M_{ZZ} spectrum is hence used as the discriminant variable in the final stage of the analysis, and the test statistic is evaluated with a binned maximum-likelihood fit of signal and background models to the observed M_{ZZ} distribution. For light Higgs masses, the observed M_{ZZ} distribution is dominated by experimental resolution effects and for example fitted as Gaussian with a standard deviation of 2–2.5 GeV (or similar bin sizes are used). Since the width of a light SM Higgs boson is 2–3 orders of magnitude smaller, one would expect that the ZWA is highly accurate. According to Eq. (2.7), the constraints on M_{ZZ} mentioned above introduce an error of order 0.1%. Invariant masses above $2\,M_Z$, where large deviations from the Breit-Wigner shape occur, are excluded by the experimental procedure. Higgs-continuum interference effects are negligible. For illustration, we compute the Higgs cross section in ZWA and off-shell including continuum interference in the vicinity of M_H, more precisely $|M_{ZZ} - M_H| < 1\,\text{GeV}$. To take into account the detector acceptance, we require $p_{T\ell} > 5\,\text{GeV}$ and $|\eta_\ell| < 2.5$. Leptons are separated using $\Delta R_{\ell\ell} > 0.1$. Following Ref. [89], we apply the cuts $76\,\text{GeV} < M_{\ell\bar{\ell},12} < 106\,\text{GeV}$ and $15\,\text{GeV} < M_{\ell\bar{\ell},34} < 115\,\text{GeV}$. The invariant mass of the same-flavour, opposite-sign lepton pair closest to M_Z is denoted by $M_{\ell\bar{\ell},12}$. $M_{\ell\bar{\ell},34}$ denotes the invariant mass of the remaining lepton pair. The γ^* singularity for vanishing virtuality is excluded by requiring $M_{\ell\bar{\ell}} > 4\,\text{GeV}$.[7] The results are displayed in Table 3.

3.2 $gg \to H \to W^-W^+ \to \ell\bar{\nu}_\ell\bar{\ell}\nu_\ell$ at $M_H = 125\,\text{GeV}$

The $WW \to 2\ell\,2\nu$ search channel has been analysed by ATLAS [91] and CMS [92] for Higgs masses in the range 110–600 GeV. We apply the standard cuts $p_{T\ell} > 20\,\text{GeV}$, $|\eta_\ell| < 2.5$, $\not{p}_T > 30\,\text{GeV}$ and $M_{\ell\ell} > 12\,\text{GeV}$. As Higgs search selection cuts, we apply the standard cuts and in addition $M_{\ell\ell} < 50\,\text{GeV}$ and $\Delta\phi_{\ell\ell} < 1.8$. Since M_{H^*} cannot be reconstructed,

[7] This cut is induced by the phase space generation.

ATLAS and CMS also use transverse mass observables M_T that aim at approximating M_{H^*}. Ref. [91] uses the transverse mass definition[8]

$$M_{T1} = \sqrt{(M_{T,\ell\ell} + \not{p}_T)^2 - (\mathbf{p}_{T,\ell\ell} + \not{\mathbf{p}}_T)^2} \tag{3.6}$$

with

$$M_{T,\ell\ell} = \sqrt{p_{T,\ell\ell}^2 + M_{\ell\ell}^2} \tag{3.7}$$

and applies a $0.75 M_H < M_{T1} < M_H$ cut for $M_H = 125\,\text{GeV}$. Ref. [92] uses the transverse mass definition

$$M_{T2} = \sqrt{2\, p_{T,\ell\ell}\, \not{p}_T (1 - \cos\Delta\phi_{\ell\ell,\text{miss}})}\,, \tag{3.8}$$

where $\Delta\phi_{\ell\ell,\text{miss}}$ is the angle between $\mathbf{p}_{T,\ell\ell}$ and $\not{\mathbf{p}}_T$, and applies a $80\ \text{GeV} < M_{T2} < M_H$ cut for $M_H = 125\,\text{GeV}$.

Cross sections are presented in Table 4. When standard cuts are applied, the phase space region where $M_{WW} > 160\,\text{GeV}$, or equivalently $M_{WW} > M_H + 7000\Gamma_H$, contributes 16% to the off-shell Higgs cross section. The error of the ZWA exceeds 15%, and interference effects are of $\mathcal{O}(10\%)$. Figs. 4 and 5 illustrate that the region with $M_{WW} > 2\,M_W$ is responsible for the inaccuracy of the ZWA as well as the unexpectedly large interference effects, in agreement with our discussion in Section 2. Fig. 6 demonstrates that finite-width effects and Higgs-continuum interference are negligible in the resonance region, i.e. $|M_{WW} - M_H| \lesssim \Gamma_H$, for a Higgs mass of 125 GeV. The Higgs search selection has additional cuts, in particular an upper bound on the invariant mass of the observed dilepton system, which significantly reduce the contribution from the region with $M_{WW} \gg 2\,M_W$, as seen in Fig. 7. The result is a substantial mitigation of the finite-width and interference effects as seen in Table 4.

We now consider the impact of cuts on transverse mass observables, which are designed to have the physical mass of the decaying parent particle (the invariant mass in the off-shell case) as upper bound [93].[9] For the process considered here, this is shown in Fig. 8. Evidently, imposing a cut $M_T < M_H$ is an effective means to suppress interference effects. This was first noticed and studied for the M_{T1} variable in Ref. [64]. In Table 4, one can see that both, M_{T1} and M_{T2}, are suitable transverse mass variables, with M_{T1} being slightly more effective. This is also borne out by the transverse mass distributions in Figs. 9 and 10. With regard to the ZWA, Table 4 shows that the application of the M_{T1} or M_{T2} cut reduces the ZWA error to the sub-percent level.

3.3 $gg \to H \to ZZ \to \ell\bar{\ell}\nu_\ell\bar{\nu}_\ell$ at $M_H = 200\,\text{GeV}$

The $ZZ \to 2\ell\,2\nu$ search channel has been analysed by ATLAS [94] and CMS [95] for Higgs masses in the range 200–600 GeV. In this section we focus on the lowest studied Higgs mass

[8] In the absence of additional observed final state particles, the expressions for M_T simplify due to $\not{\mathbf{p}}_T = -\mathbf{p}_{T,\ell\ell}$.

[9] We note that M_{T1} is referred to as M_T^{true} in Ref. [93].

	$gg\ (\to H) \to W^-W^+ \to \ell\bar{\nu}_\ell\bar{\ell}\nu_\ell$						
	σ [fb], pp, $\sqrt{s} = 8\,\text{TeV}$, $M_H = 125\,\text{GeV}$				ZWA	interference	
selection cuts	H_{ZWA}	H_{offshell}	cont	$\lvert H_{\text{ofs}}+\text{cont}\rvert^2$	R_0	R_1	R_2
standard cuts	2.707(3)	3.225(3)	10.493(5)	12.241(8)	0.839(2)	0.8923(7)	0.542(3)
Higgs search cuts	1.950(1)	1.980(1)	2.705(2)	4.497(3)	0.9850(7)	0.9599(7)	0.905(2)
$0.75M_H < M_{T1} < M_H$	1.7726(9)	1.779(1)	0.6443(9)	2.383(2)	0.9966(8)	0.983(1)	0.977(2)
80 GeV $< M_{T2} < M_H$	1.7843(9)	1.794(1)	0.955(1)	2.687(3)	0.9944(8)	0.977(1)	0.965(2)

Table 4. Cross sections for $gg\ (\to H) \to W^-W^+ \to \ell\bar{\nu}_\ell\bar{\ell}\nu_\ell$ for $M_H = 125\,\text{GeV}$ with standard cuts, Higgs search cuts and additional transverse mass cut (either on M_{T1} or M_{T2}). Standard cuts: $p_{T\ell} > 20\,\text{GeV}$, $|\eta_\ell| < 2.5$, $\not{p}_T > 30\,\text{GeV}$, $M_{\ell\ell} > 12\,\text{GeV}$. Higgs search cuts: standard cuts and $M_{\ell\ell} < 50\,\text{GeV}$, $\Delta\phi_{\ell\ell} < 1.8$. M_{T1} and M_{T2} are defined in Eqs. (3.6) and (3.8) in the main text. Other details as in Table 3.

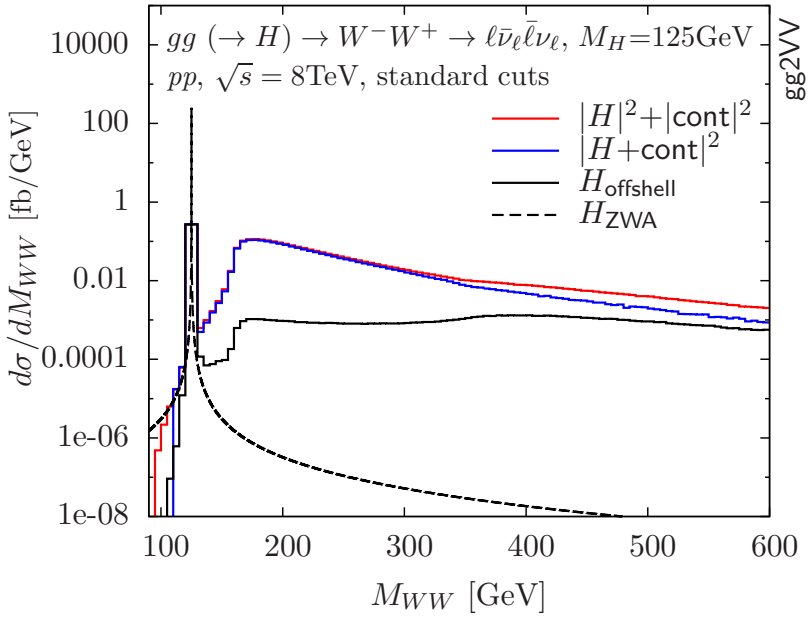

Figure 4. M_{WW} distributions for $gg\ (\to H) \to W^-W^+ \to \ell\bar{\nu}_\ell\bar{\ell}\nu_\ell$ in pp collisions at $\sqrt{s} = 8\,\text{TeV}$ for $M_H = 125\,\text{GeV}$ and $\Gamma_H = 0.004434\,\text{GeV}$ calculated at LO with gg2VV. The ZWA distribution (black, dashed) as defined in Eq. (3.2) in the main text, the off-shell Higgs distribution (black, solid), the $d\sigma(|\mathcal{M}_H + \mathcal{M}_{\text{cont}}|^2)/dM_{WW}$ distribution (blue) and the $d\sigma(|\mathcal{M}_H|^2 + |\mathcal{M}_{\text{cont}}|^2)/dM_{WW}$ distribution (red) are shown. Standard cuts are applied: $p_{T\ell} > 20\,\text{GeV}$, $|\eta_\ell| < 2.5$, $\not{p}_T > 30\,\text{GeV}$, $M_{\ell\ell} > 12\,\text{GeV}$. Differential cross sections for a single lepton flavour combination are displayed. No flavour summation is carried out for charged leptons or neutrinos.

of 200 GeV with $\Gamma_H/M_H = 0.7\%$. Note that M_H is slightly above the Z pair production threshold. A clean separation of the Higgs resonance and the region with large continuum background is thus not possible. We apply the Higgs search cuts $p_{T\ell} > 20\,\text{GeV}$, $|\eta_\ell| < 2.5$, $76\,\text{GeV} < M_{\ell\ell} < 106\,\text{GeV}$, $\not{p}_T > 10\,\text{GeV}$ and $\Delta\phi_{\ell\ell} > 1$. Refs. [94] and [95] use a transverse mass distribution as final discriminant in searching for an excess of data over the SM background expectation. Ref. [95] employs the transverse mass variable first proposed in

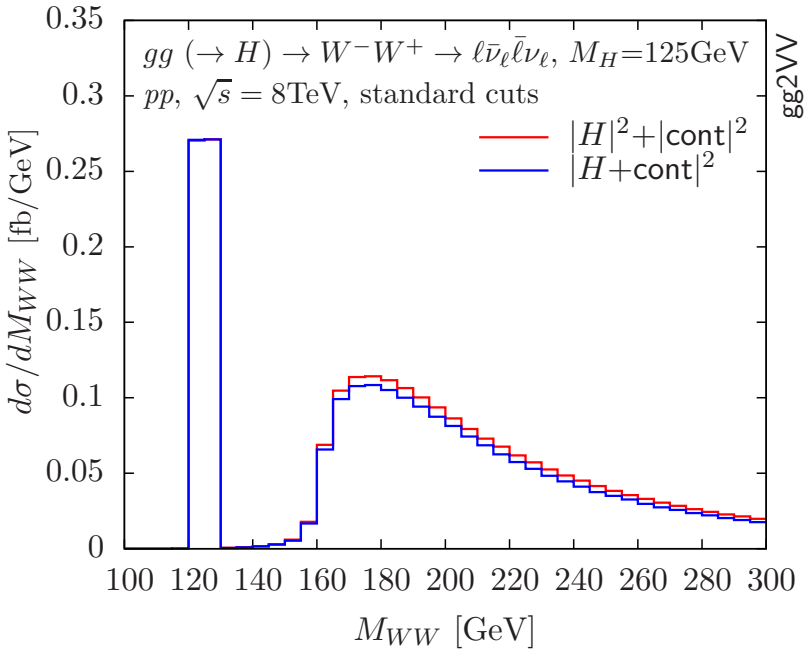

Figure 5. M_{WW} distributions for $gg\ (\to H) \to W^-W^+ \to \ell\bar{\nu}_\ell\bar{\ell}\nu_\ell$ for $M_H = 125\,\text{GeV}$. Interference effects in the region of the Higgs resonance and the W-pair threshold are shown. Details as in Fig. 4.

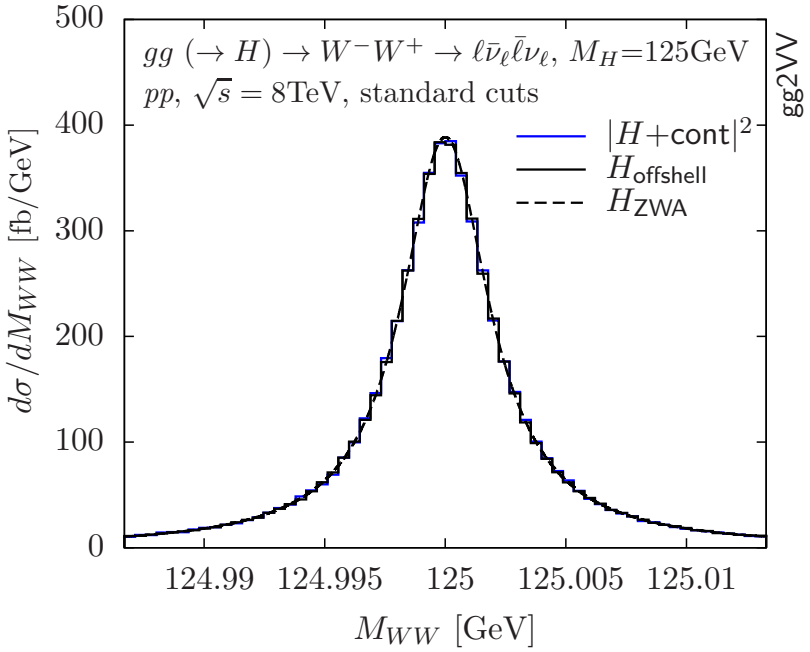

Figure 6. M_{WW} distributions for $gg\ (\to H) \to W^-W^+ \to \ell\bar{\nu}_\ell\bar{\ell}\nu_\ell$ for $M_H = 125\,\text{GeV}$. Off-shell and interference effects in the vicinity of the Higgs resonance are shown. Details as in Fig. 4.

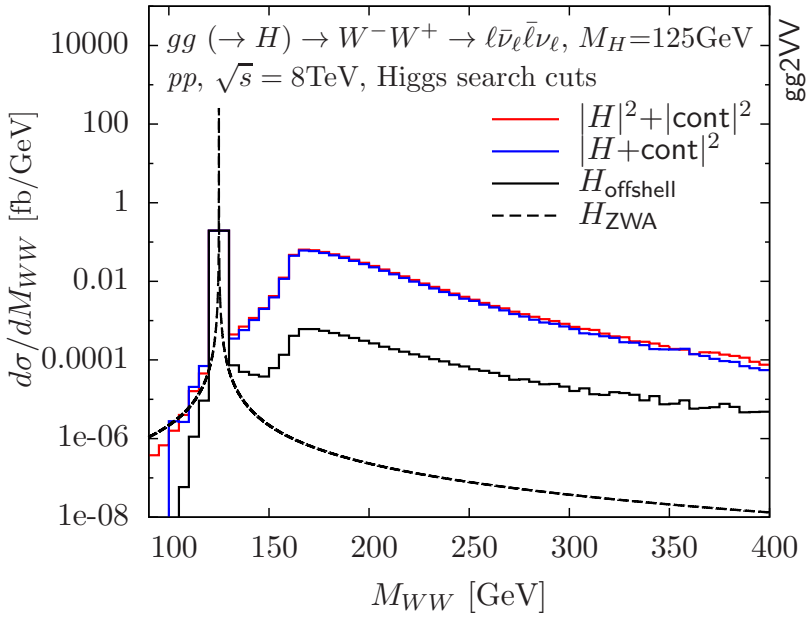

Figure 7. M_{WW} distributions for $gg\ (\to H) \to W^-W^+ \to \ell\bar{\nu}_\ell\bar{\ell}\nu_\ell$ for $M_H = 125\,\text{GeV}$. Higgs search cuts are applied: $p_{T\ell} > 20\,\text{GeV}$, $|\eta_\ell| < 2.5$, $\not{p}_T > 30\,\text{GeV}$, $12\,\text{GeV} < M_{\ell\ell} < 50\,\text{GeV}$, $\Delta\phi_{\ell\ell} < 1.8$. Other details as in Fig. 4.

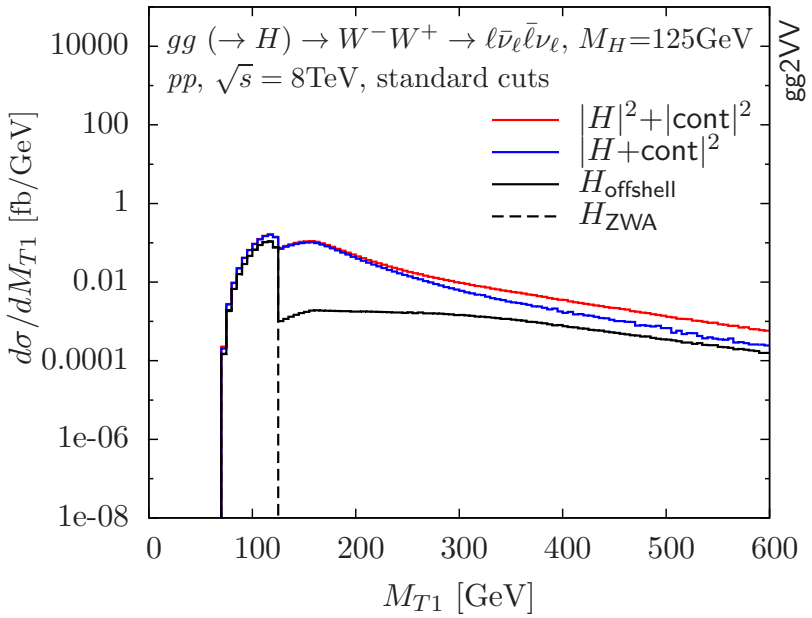

Figure 8. Transverse mass distributions for $gg\ (\to H) \to W^-W^+ \to \ell\bar{\nu}_\ell\bar{\ell}\nu_\ell$ for $M_H = 125\,\text{GeV}$. M_{T1} is defined in Eq. (3.6) in the main text. Other details as in Fig. 4.

Ref. [96] for the weak boson fusion $H \to WW$ channel:

$$M_{T3} = \sqrt{(M_{T,\ell\ell} + \not{M}_T)^2 - (\mathbf{p}_{T,\ell\ell} + \not{\mathbf{p}}_T)^2} \tag{3.9}$$

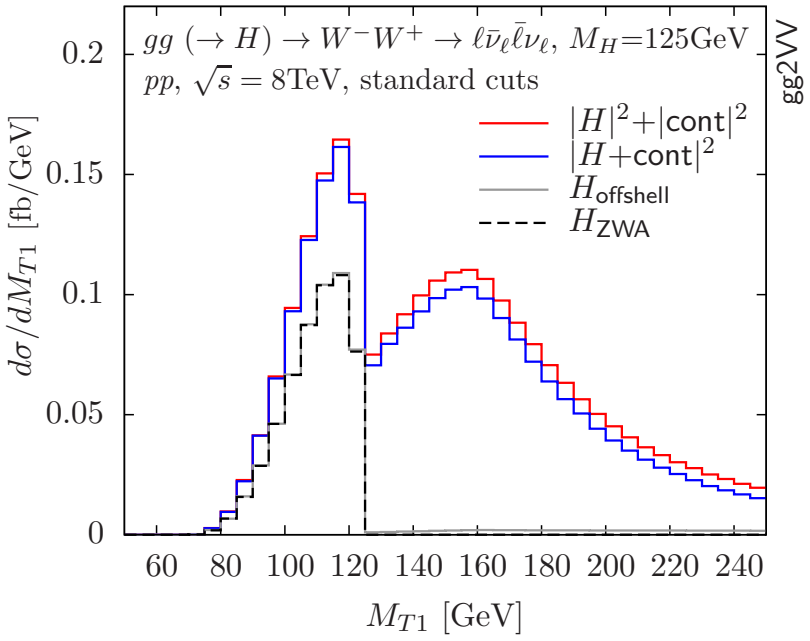

Figure 9. M_{T1} distributions for $gg\ (\to H) \to W^-W^+ \to \ell\bar{\nu}_\ell\bar{\ell}\nu_\ell$ for $M_H = 125\,\text{GeV}$. Off-shell and interference effects in the region of the Higgs resonance and the W-pair threshold are shown. M_{T1} is defined in Eq. (3.6) in the main text. Other details as in Fig. 4.

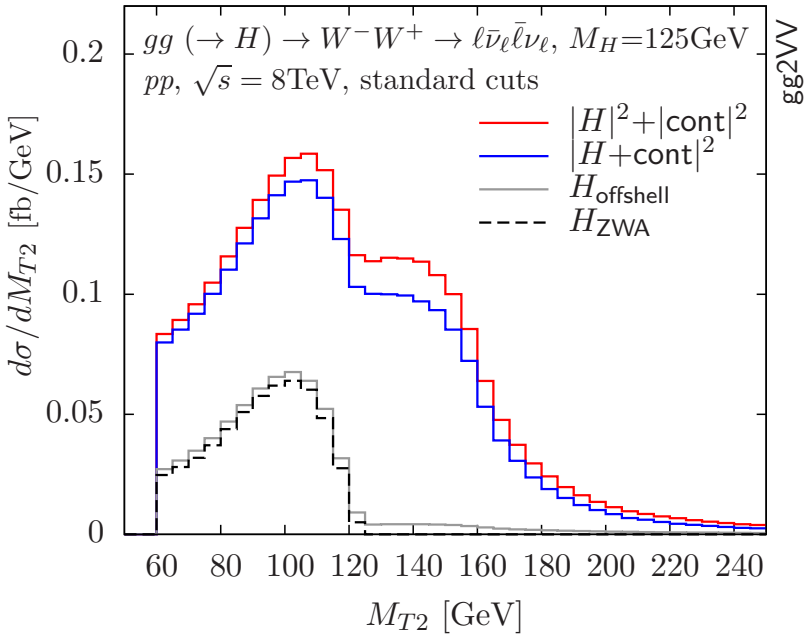

Figure 10. M_{T2} distributions for $gg\ (\to H) \to W^-W^+ \to \ell\bar{\nu}_\ell\bar{\ell}\nu_\ell$ for $M_H = 125\,\text{GeV}$. Off-shell and interference effects in the region of the Higgs resonance and the W-pair threshold are shown. M_{T2} is defined in Eq. (3.8) in the main text. Other details as in Fig. 4.

$gg\ (\to H) \to ZZ \to \ell\bar{\ell}\nu_\ell\bar{\nu}_\ell$						
σ [fb], pp, $\sqrt{s} = 8\,\text{TeV}$, $M_H = 200\,\text{GeV}$				ZWA	interference	
H_{ZWA}	H_{offshell}	cont	$\lvert H_{\text{ofs}}+\text{cont}\rvert^2$	R_0	R_1	R_2
2.0357(8)	2.0608(9)	1.1888(6)	3.380(2)	0.9878(6)	1.0400(7)	1.063(1)

Table 5. Cross sections for $gg\ (\to H) \to ZZ \to \ell\bar{\ell}\nu_\ell\bar{\nu}_\ell$ for $M_H = 200\,\text{GeV}$ and $\Gamma_H = 1.428\,\text{GeV}$. Applied cuts: $p_{T\ell} > 20\,\text{GeV}$, $|\eta_\ell| < 2.5$, $76\,\text{GeV} < M_{\ell\ell} < 106\,\text{GeV}$, $\not{p}_T > 10\,\text{GeV}$, $\Delta\phi_{\ell\ell} > 1$. Other details as in Table 3.

with $M_{T,\ell\ell}$ defined in Eq. (3.7) and

$$\not{M}_T = \sqrt{\not{p}_T^2 + M_{\ell\ell}^2} \tag{3.10}$$

Note that M_{T3}, unlike M_{T1} and M_{T2}, does not have a kinematic edge at M_{H^*}. The variable used in Ref. [94] is obtained by replacing $M_{\ell\ell}$ with M_Z in the definition of M_{T3}, which causes only minor differences for $M_H > 2M_Z$. No M_T cut is applied in the analyses.

In Table 5, cross section results are given. The ZWA is accurate at the percent level. Fig. 11 reveals that the off-shell enhancement of the high M_{H^*} tail is moderate. Higgs-continuum interference is constructive and of $\mathcal{O}(5\%)$. Significant interference occurs in the vicinity of the Higgs resonance as shown in Figs. 12 and 13. ZZ interference effects are comparable to WW interference effects for similar Higgs masses [62, 64]. The M_{T3} distributions displayed in Fig. 14 show that sizable ZWA deviations occur at the differential level.

3.4 $gg \to H \to ZZ \to \ell\bar{\ell}\nu_\ell\bar{\nu}_\ell$ at $M_H = 125\,\text{GeV}$

Given the rapid increase in integrated luminosity at the LHC, the $ZZ \to 2\ell\,2\nu$ mode could also be of interest at $M_H = 125\,\text{GeV}$. We therefore extend our study to this Higgs mass. The following selection cuts are applied: $p_{T\ell} > 20\,\text{GeV}$, $|\eta_\ell| < 2.5$, $76\,\text{GeV} < M_{\ell\ell} < 106\,\text{GeV}$ and $\not{p}_T > 10\,\text{GeV}$. As seen in Fig. 15, the off-shell enhancement of the high M_{H^*} tail is particularly pronounced. In Table 6, cross section results are given. The phase space region where $M_{ZZ} > 180\,\text{GeV}$, or equivalently $M_{ZZ} > M_H + 12000\Gamma_H$, contributes 37% to the off-shell Higgs cross section. The ZWA underestimates the Higgs cross section by a similar amount. Figs. 15 and 16 illustrate that the region with $M_{ZZ} > 2\,M_Z$ is also responsible for interference effects of $\mathcal{O}(10\%)$. Fig. 17 demonstrates that finite-width effects and Higgs-continuum interference are negligible in the resonance region.

To mitigate the impact of the M_{H^*} region with large ZWA deviations and Higgs-continuum interference, we propose to employ a $M_{T1} < M_H$ cut. With this cut, the off-shell and interference effects (R_1) are reduced to the 2% level. The M_{T1} distribution displayed in Fig. 18 shows that the contamination of the $M_{T1} < M_H$ region from the interference-inducing $M_{H^*} > 2\,M_Z$ region is more severe than in the WW case (see Fig. 9).

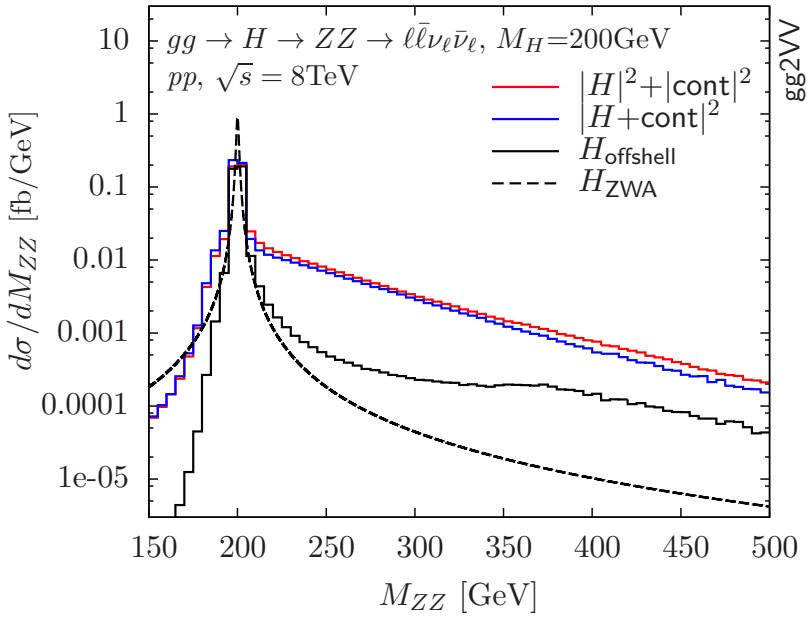

Figure 11. M_{ZZ} distributions for $gg \to H \to ZZ \to \ell\bar{\ell}\nu_\ell\bar{\nu}_\ell$ for $M_H = 200\,\text{GeV}$ and $\Gamma_H = 1.428\,\text{GeV}$. Applied cuts: $p_{T\ell} > 20\,\text{GeV}$, $|\eta_\ell| < 2.5$, $76\,\text{GeV} < M_{\ell\ell} < 106\,\text{GeV}$, $\not{p}_T > 10\,\text{GeV}$, $\Delta\phi_{\ell\ell} > 1$. Other details as in Fig. 4.

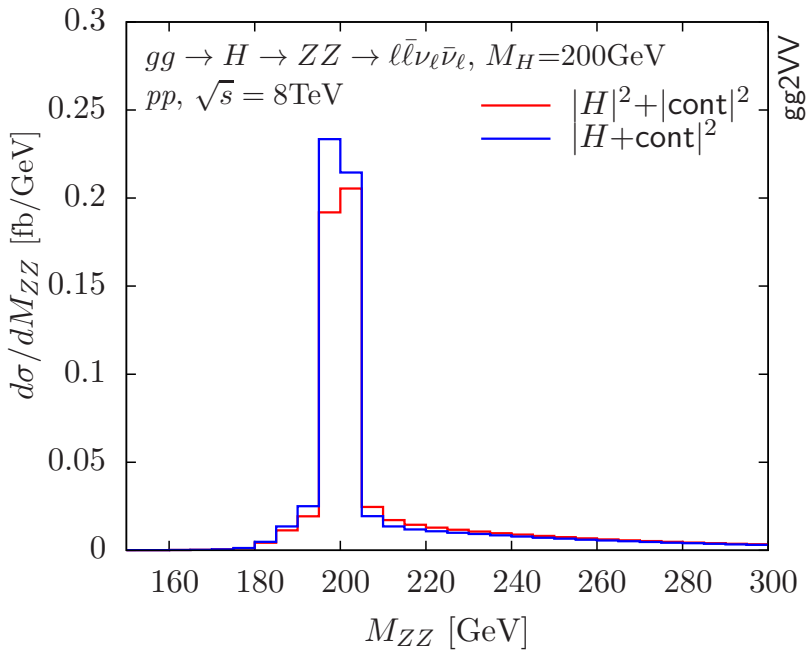

Figure 12. M_{ZZ} distributions for $gg \to H \to ZZ \to \ell\bar{\ell}\nu_\ell\bar{\nu}_\ell$ for $M_H = 200\,\text{GeV}$. Interference effects in the region of the Higgs resonance and the Z-pair threshold are shown. Details as in Fig. 11.

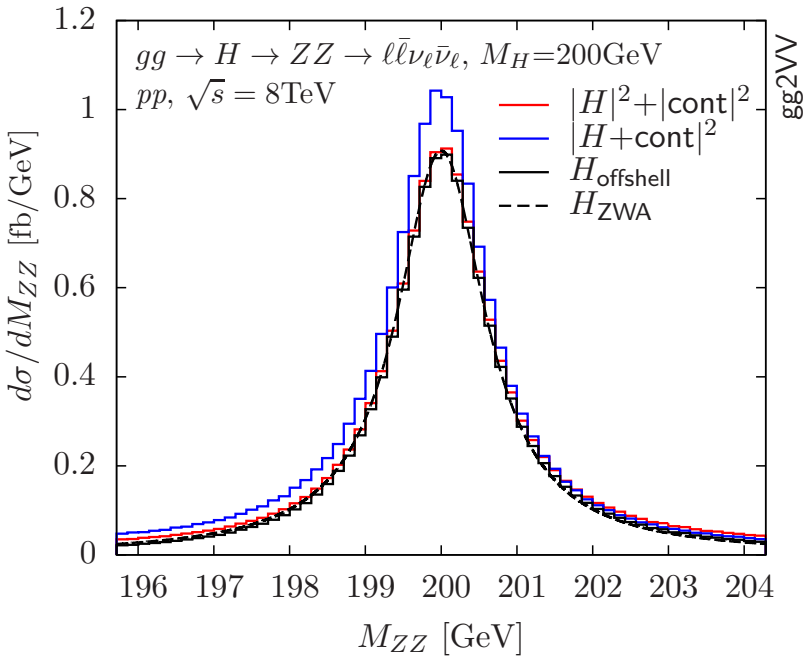

Figure 13. M_{ZZ} distributions for $gg \to H \to ZZ \to \ell\bar{\ell}\nu_\ell\bar{\nu}_\ell$ for $M_H = 200\,\text{GeV}$. Off-shell and interference effects in the vicinity of the Higgs resonance are shown. Details as in Fig. 11.

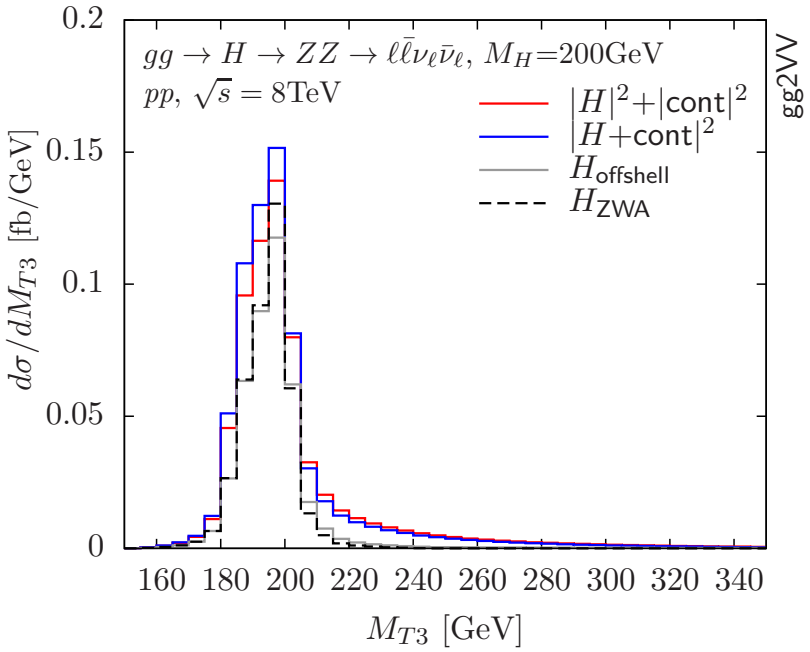

Figure 14. Transverse mass distributions for $gg \to H \to ZZ \to \ell\bar{\ell}\nu_\ell\bar{\nu}_\ell$ for $M_H = 200\,\text{GeV}$. M_{T3} is defined in Eq. (3.9) in the main text. Other details as in Fig. 11.

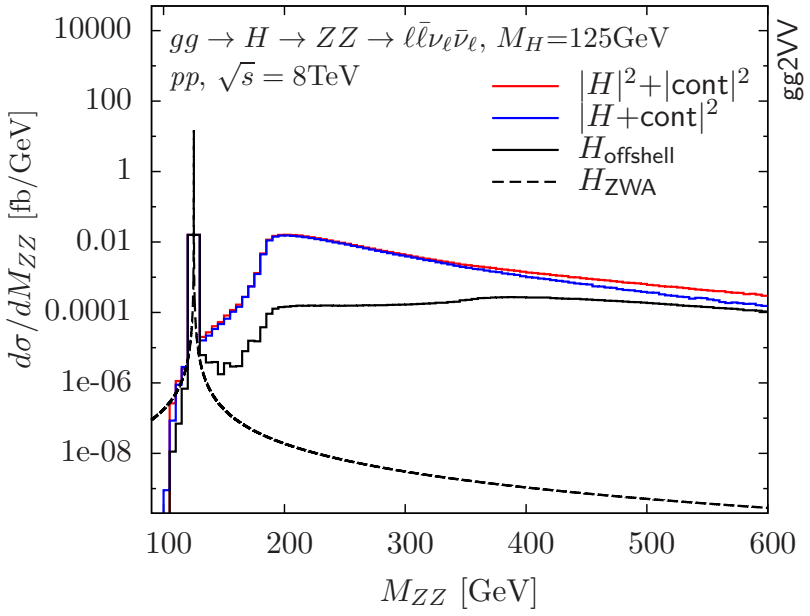

Figure 15. M_{ZZ} distributions for $gg \to H \to ZZ \to \ell\bar{\ell}\nu_\ell\bar{\nu}_\ell$ for $M_H = 125\,\text{GeV}$. Applied cuts: $p_{T\ell} > 20\,\text{GeV}$, $|\eta_\ell| < 2.5$, $76\,\text{GeV} < M_{\ell\ell} < 106\,\text{GeV}$, $\not{p}_T > 10\,\text{GeV}$. Other details as in Fig. 4.

	$gg\ (\to H) \to ZZ \to \ell\bar{\ell}\nu_\ell\bar{\nu}_\ell$						
	σ [fb], pp, $\sqrt{s} = 8\,\text{TeV}$, $M_H = 125\,\text{GeV}$				ZWA	interference	
M_T cut	$H_{\rm ZWA}$	$H_{\rm offshell}$	cont	$\lvert H_{\rm ofs}$+cont$\rvert^2$	R_0	R_1	R_2
none	0.1593(2)	0.2571(2)	1.5631(7)	1.6376(9)	0.6196(7)	0.8997(6)	0.290(5)
$M_{T1} < M_H$	0.1593(2)	0.1625(2)	0.4197(5)	0.5663(6)	0.980(2)	0.973(2)	0.902(5)

Table 6. Cross sections for $gg\ (\to H) \to ZZ \to \ell\bar{\ell}\nu_\ell\bar{\nu}_\ell$ for $M_H = 125\,\text{GeV}$ without and with transverse mass cut. Applied cuts: $p_{T\ell} > 20\,\text{GeV}$, $|\eta_\ell| < 2.5$, $76\,\text{GeV} < M_{\ell\ell} < 106\,\text{GeV}$, $\not{p}_T > 10\,\text{GeV}$. Other details as in Table 3.

4 Conclusions

In the Higgs search at the LHC, a light Higgs boson is not excluded by experimental data. In the mass range $115\,\text{GeV} \lesssim M_H \lesssim 130\,\text{GeV}$, one has $\Gamma_H/M_H < 10^{-4}$ for the SM Higgs boson. We have shown for inclusive cross sections and cross sections with experimental selection cuts that the ZWA is in general not adequate and the error estimate $\mathcal{O}(\Gamma_H/M_H)$ is not reliable for a light Higgs boson. The inclusion of off-shell contributions is essential to obtain an accurate Higgs signal normalisation at the 1% precision level. We have traced this back to the dependence of the decay (and to a lesser degree production) matrix element on the Higgs virtuality q^2. For the $H \to WW, ZZ$ decay modes we find that above the weak-boson pair production threshold the $(q^2)^2$ dependence of the decay matrix element compensates the q^2-dependence of the Higgs propagator, which results in a significantly enhanced off-shell cross section in comparison to the ZWA cross section, when this phase

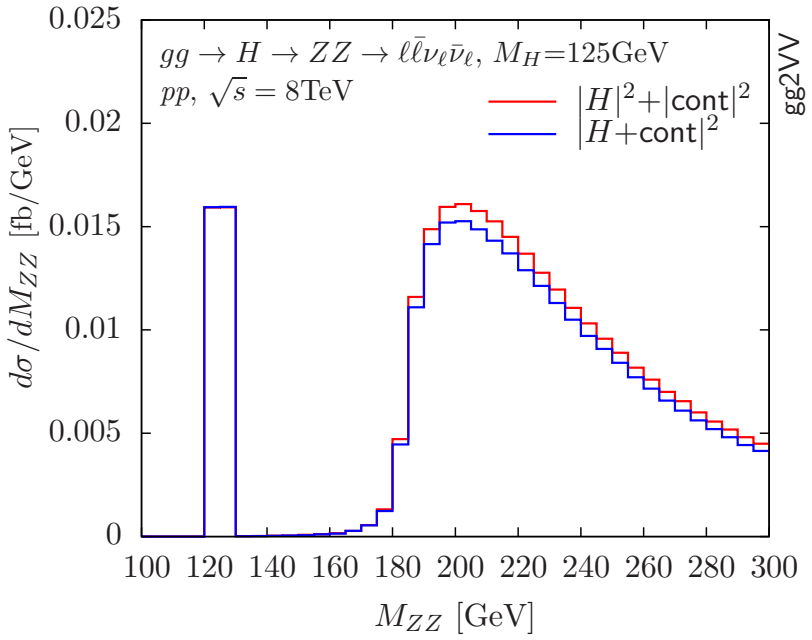

Figure 16. M_{ZZ} distributions for $gg \to H \to ZZ \to \ell\bar{\ell}\nu_\ell\bar{\nu}_\ell$ for $M_H = 125\,\text{GeV}$. Interference effects in the region of the Higgs resonance and the Z-pair threshold are shown. Details as in Fig. 15.

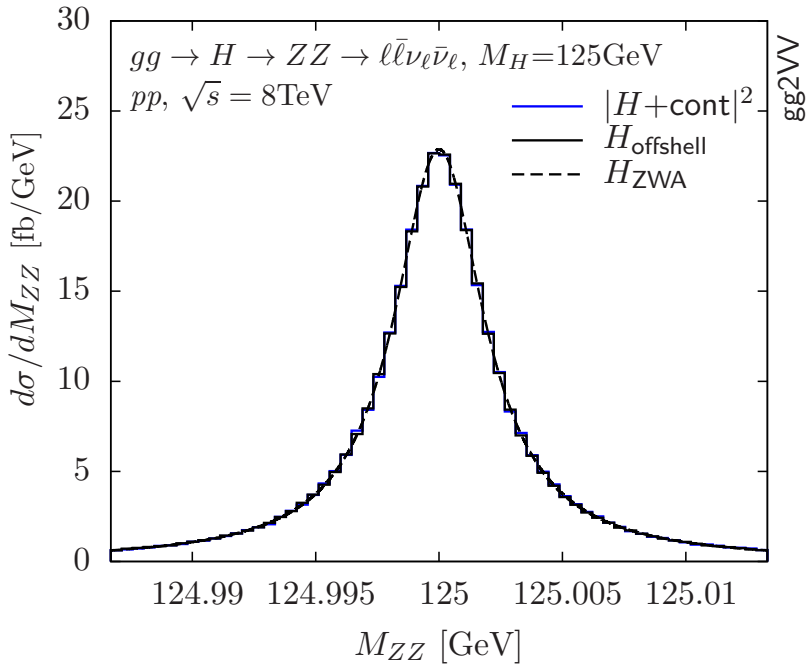

Figure 17. M_{ZZ} distributions for $gg \to H \to ZZ \to \ell\bar{\ell}\nu_\ell\bar{\nu}_\ell$ for $M_H = 125\,\text{GeV}$. Off-shell and interference effects in the vicinity of the Higgs resonance are shown. Details as in Fig. 15.

space region, which is also affected by sizable Higgs-continuum interference, contributes.

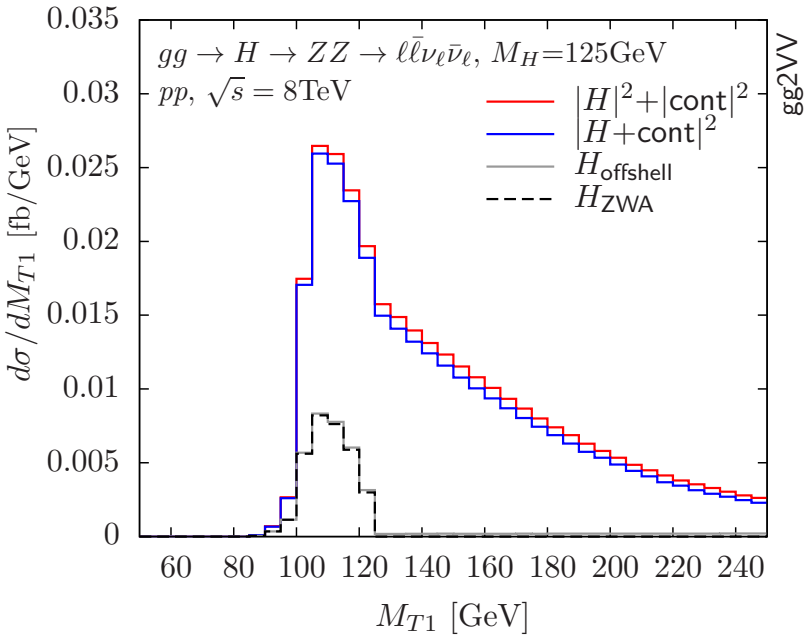

Figure 18. Transverse mass distributions for $gg \to H \to ZZ \to \ell\bar{\ell}\nu_\ell\bar{\nu}_\ell$ for $M_H = 125\,\text{GeV}$. M_{T1} is defined in Eq. (3.6) in the main text. Other details as in Fig. 15.

As shape of the enhancement above $2\,M_V$, we find a "plateau" up to the $t\bar{t}$-threshold and an exponential decrease beyond it. The total $gg \to H \to VV$ cross section thus receives an $\mathcal{O}(10\%)$ off-shell correction. We have further illustrated that the region above $2\,M_V$ is responsible for $\mathcal{O}(10\%)$ Higgs-continuum interference effects, which, due to the off-shell enhanced tail, can have a significant impact even for $M_H \ll 2\,M_V$. We find that in the vicinity of the Higgs resonance finite-width and Higgs-continuum interference effects are negligible for $M_H \ll 2\,M_V$, while for $M_H = 200$ GeV this is not the case.

For weak boson decays that permit the reconstruction of the invariant Higgs mass, the enhanced region is eliminated by the experimental procedure as long as $M_H \ll 2\,M_V$. For channels where the Higgs invariant mass cannot be reconstructed, we have illustrated that $H \to WW$ search selection cuts for a light Higgs boson reduce the contribution of the off-shell enhanced tail, and that the tail can effectively be excluded for the $H \to WW$ as well as $H \to ZZ$ decay mode by using transverse mass observables (M_T) that approximate the Higgs invariant mass and applying a $M_T < M_H$ cut. We predict that the weak boson fusion $H \to VV$ channels also exhibit an off-shell enhanced tail, since the effect is primarily caused by the Higgs decay matrix element. It is worth noting that we make no statement about the observability of a large invariant mass signal due to a low-mass Higgs boson, which is hampered by the huge background and interference effects.

After the 5σ-observation of a SM-like Higgs signal at $M_H \approx 125$–126 GeV reported by ATLAS and CMS in a recent seminar, the next step in the analysis will be the extraction of the Higgs couplings and properties. This study will initially be performed using the ZWA with a consequent error of $\mathcal{O}(5\%)$ on the couplings. Although this is still tolerable

with current statistics, the results presented above make it clear that off-shell effects have to be included in future analyses.

In summary, we have elucidated the inadequacy of the ZWA in general and the existence of an enhanced tail in the Higgs invariant mass distribution of a light Higgs boson that decays to a weak-boson pair in particular, which makes off-shell calculations mandatory and will lead to significant errors when the ZWA is used, unless the affected region of invariant masses above the weak-boson-pair threshold is excluded with selection cuts. The latter is also motivated by the fact that intuitively one would not like to assign events with large invariant mass to a low-mass Higgs signal, not least because they are affected by large signal-background interference. As consequence of our findings, we recommend that the explicit or implicit application of the ZWA in experimental studies be identified and corrected for.

Acknowledgments

We would like to thank the conveners and members of the LHC Higgs Cross Section Working Group for stimulating and informative discussions. N.K. would like to thank M. Rodgers for useful comparisons. G.P.'s work is supported by MIUR under contract 2001023713_006 and by Compagnia di San Paolo under contract ORTO11TPXK. Financial support from the Higher Education Funding Council for England, the Science and Technology Facilities Council and the Institute for Particle Physics Phenomenology, Durham, is gratefully acknowledged by N.K.

References

[1] P. W. Higgs, *Broken symmetries, massless particles and gauge fields*, Phys. Lett. **12** (1964) 132.

[2] P. W. Higgs, *Broken symmetries and the masses of gauge bosons*, Phys. Rev. Lett. **13** (1964) 508.

[3] P. W. Higgs, *Spontaneous symmetry breakdown without massless bosons*, Phys. Rev. **145** (1966) 1156.

[4] F. Englert and R. Brout, *Broken symmetry and the mass of gauge vector mesons*, Phys. Rev. Lett. **13** (1964) 321.

[5] G. S. Guralnik, C. R. Hagen and T. W. B. Kibble, *Global conservation laws and massless particles*, Phys. Rev. Lett. **13** (1964) 585.

[6] R. Barate *et al.* [LEP Working Group for Higgs boson searches and ALEPH and DELPHI and L3 and OPAL Collaborations], *Search for the Standard Model Higgs boson at LEP*, Phys. Lett. B **565** (2003) 61 [hep-ex/0306033].

[7] C. a. D. C. a. t. T. N. P. a. H. W. Group [Tevatron New Physics Higgs Working Group and CDF and D0 Collaborations], *Updated combination of CDF and D0 searches for Standard Model Higgs boson production with up to 10.0 fb^{-1} of data*, arXiv:1207.0449 [hep-ex].

[8] S. Chatrchyan *et al.* [CMS Collaboration], *Combined results of searches for the Standard Model Higgs boson in pp collisions at* $\sqrt{s} = 7$ *TeV*, Phys. Lett. B **710** (2012) 26 [arXiv:1202.1488 [hep-ex]].

[9] G. Aad *et al.* [ATLAS Collaboration], *Combined search for the Standard Model Higgs boson in pp collisions at* $\sqrt{s} = 7$ *TeV with the ATLAS detector*, arXiv:1207.0319 [hep-ex].

[10] H. M. Georgi, S. L. Glashow, M. E. Machacek and D. V. Nanopoulos, *Higgs bosons from two gluon annihilation in proton proton collisions*, Phys. Rev. Lett. **40** (1978) 692.

[11] S. Dawson, *Radiative corrections to Higgs boson production*, Nucl. Phys. B **359** (1991) 283.

[12] A. Djouadi, M. Spira and P. M. Zerwas, *Production of Higgs bosons in proton colliders: QCD corrections*, Phys. Lett. B **264** (1991) 440.

[13] D. Graudenz, M. Spira and P. M. Zerwas, *QCD corrections to Higgs boson production at proton proton colliders*, Phys. Rev. Lett. **70** (1993) 1372.

[14] M. Spira, A. Djouadi, D. Graudenz and P. M. Zerwas, *Higgs boson production at the LHC*, Nucl. Phys. B **453** (1995) 17 [hep-ph/9504378].

[15] R. V. Harlander and W. B. Kilgore, *Next-to-next-to-leading order Higgs production at hadron colliders*, Phys. Rev. Lett. **88** (2002) 201801 [hep-ph/0201206].

[16] C. Anastasiou and K. Melnikov, *Higgs boson production at hadron colliders in NNLO QCD*, Nucl. Phys. B **646** (2002) 220 [arXiv:hep-ph/0207004].

[17] V. Ravindran, J. Smith and W. L. van Neerven, *NNLO corrections to the total cross section for Higgs boson production in hadron-hadron collisions*, Nucl. Phys. B **665** (2003) 325 [arXiv:hep-ph/0302135].

[18] S. Catani, D. de Florian, M. Grazzini and P. Nason, *Soft gluon resummation for Higgs boson production at hadron colliders*, JHEP **0307** (2003) 028 [hep-ph/0306211].

[19] D. de Florian, G. Ferrera, M. Grazzini and D. Tommasini, *Transverse-momentum resummation: Higgs boson production at the Tevatron and the LHC*, JHEP **1111** (2011) 064 [arXiv:1109.2109 [hep-ph]].

[20] S. Moch and A. Vogt, *Higher-order soft corrections to lepton pair and Higgs boson production*, Phys. Lett. B **631** (2005) 48 [hep-ph/0508265].

[21] E. Laenen and L. Magnea, *Threshold resummation for electroweak annihilation from DIS data*, Phys. Lett. B **632** (2006) 270 [hep-ph/0508284].

[22] A. Idilbi, X. -d. Ji, J. -P. Ma and F. Yuan, *Threshold resummation for Higgs production in effective field theory*, Phys. Rev. D **73** (2006) 077501 [hep-ph/0509294].

[23] V. Ravindran, *On Sudakov and soft resummations in QCD*, Nucl. Phys. B **746** (2006) 58 [hep-ph/0512249].

[24] V. Ravindran, *Higher-order threshold effects to inclusive processes in QCD*, Nucl. Phys. B **752** (2006) 173 [hep-ph/0603041].

[25] V. Ahrens, T. Becher, M. Neubert and L. L. Yang, *Renormalization-group improved prediction for Higgs production at hadron colliders*, Eur. Phys. J. C **62** (2009) 333 [arXiv:0809.4283 [hep-ph]].

[26] C. Anastasiou, K. Melnikov and F. Petriello, *Higgs boson production at hadron colliders: differential cross sections through next-to-next-to-leading order*, Phys. Rev. Lett. **93** (2004) 262002 [arXiv:hep-ph/0409088].

[27] S. Catani and M. Grazzini, *A NNLO subtraction formalism in hadron collisions and its application to Higgs boson production at the LHC*, Phys. Rev. Lett. **98** (2007) 222002 [arXiv:hep-ph/0703012].

[28] S. Marzani, R. D. Ball, V. Del Duca, S. Forte and A. Vicini, *Higgs production via gluon-gluon fusion with finite top mass beyond next-to-leading order*, Nucl. Phys. B **800** (2008) 127 [arXiv:0801.2544 [hep-ph]].

[29] R. V. Harlander and K. J. Ozeren, *Top mass effects in Higgs production at next-to-next-to-leading order QCD: Virtual corrections*, Phys. Lett. B **679** (2009) 467 [arXiv:0907.2997 [hep-ph]].

[30] A. Pak, M. Rogal and M. Steinhauser, *Virtual three-loop corrections to Higgs boson production in gluon fusion for finite top quark mass*, Phys. Lett. B **679** (2009) 473 [arXiv:0907.2998 [hep-ph]].

[31] R. V. Harlander and K. J. Ozeren, *Finite top mass effects for hadronic Higgs production at next-to-next-to-leading order*, JHEP **0911** (2009) 088 [arXiv:0909.3420 [hep-ph]].

[32] A. Pak, M. Rogal and M. Steinhauser, *Finite top quark mass effects in NNLO Higgs boson production at LHC*, JHEP **1002** (2010) 025 [arXiv:0911.4662 [hep-ph]].

[33] R. V. Harlander, H. Mantler, S. Marzani and K. J. Ozeren, *Higgs production in gluon fusion at next-to-next-to-leading order QCD for finite top mass*, Eur. Phys. J. C **66** (2010) 359 [arXiv:0912.2104 [hep-ph]].

[34] J. Baglio and A. Djouadi, *Higgs production at the lHC*, JHEP **1103** (2011) 055 [arXiv:1012.0530 [hep-ph]].

[35] A. Djouadi and P. Gambino, *Leading electroweak correction to Higgs boson production at proton colliders*, Phys. Rev. Lett. **73** (1994) 2528 [hep-ph/9406432].

[36] U. Aglietti, R. Bonciani, G. Degrassi and A. Vicini, *Two loop light fermion contribution to Higgs production and decays*, Phys. Lett. B **595** (2004) 432 [hep-ph/0404071].

[37] G. Degrassi and F. Maltoni, *Two-loop electroweak corrections to Higgs production at hadron colliders*, Phys. Lett. B **600** (2004) 255 [hep-ph/0407249].

[38] S. Actis, G. Passarino, C. Sturm and S. Uccirati, *NLO electroweak corrections to Higgs boson production at hadron colliders*, Phys. Lett. B **670** (2008) 12 [arXiv:0809.1301 [hep-ph]].

[39] S. Actis, G. Passarino, C. Sturm and S. Uccirati, *NNLO computational techniques: the cases $H \to \gamma\gamma$ and $H \to gg$*, Nucl. Phys. B **811** (2009) 182 [arXiv:0809.3667 [hep-ph]].

[40] V. Ahrens, T. Becher, M. Neubert and L. L. Yang, *Updated predictions for Higgs production at the Tevatron and the LHC*, Phys. Lett. B **698** (2011) 271 [arXiv:1008.3162 [hep-ph]].

[41] W. -Y. Keung and F. J. Petriello, *Electroweak and finite quark-mass effects on the Higgs boson transverse momentum distribution*, Phys. Rev. D **80** (2009) 013007 [arXiv:0905.2775 [hep-ph]].

[42] O. Brein, *Electroweak and bottom quark contributions to Higgs boson plus jet production*, Phys. Rev. D **81** (2010) 093006 [arXiv:1003.4438 [hep-ph]].

[43] C. Anastasiou, R. Boughezal and F. Petriello, *Mixed QCD-electroweak corrections to Higgs boson production in gluon fusion*, JHEP **0904** (2009) 003 [arXiv:0811.3458 [hep-ph]].

[44] D. de Florian and M. Grazzini, *Higgs production through gluon fusion: Updated cross sections at the Tevatron and the LHC*, Phys. Lett. B **674** (2009) 291 [arXiv:0901.2427 [hep-ph]].

[45] S. Dittmaier *et al.* [LHC Higgs Cross Section Working Group Collaboration], *Handbook of LHC Higgs Cross Sections: 1. Inclusive observables*, arXiv:1101.0593 [hep-ph].

[46] C. Anastasiou, S. Buehler, F. Herzog and A. Lazopoulos, *Total cross section for Higgs boson hadroproduction with anomalous Standard Model interactions*, JHEP **1112** (2011) 058 [arXiv:1107.0683 [hep-ph]].

[47] C. Anastasiou, S. Buehler, F. Herzog and A. Lazopoulos, *Inclusive Higgs boson cross-section for the LHC at 8 TeV*, JHEP **1204** (2012) 004 [arXiv:1202.3638 [hep-ph]].

[48] D. de Florian and M. Grazzini, *Higgs production at the LHC: updated cross sections at* $\sqrt{s} = 8$ *TeV*, arXiv:1206.4133 [hep-ph].

[49] C. Anastasiou, G. Dissertori and F. Stockli, *NNLO QCD predictions for the* $H \to WW \to \ell\nu\ell\nu$ *signal at the LHC*, JHEP **0709** (2007) 018 [arXiv:0707.2373 [hep-ph]].

[50] M. Grazzini, *NNLO predictions for the Higgs boson signal in the* $H \to WW \to \ell\nu\ell\nu$ *and* $H \to ZZ \to 4\ell$ *decay channels*, JHEP **0802** (2008) 043 [arXiv:0801.3232 [hep-ph]].

[51] S. Dittmaier, C. Mariotti, G. Passarino, R. Tanaka, S. Alekhin, J. Alwall and E. A. Bagnaschi *et al.*, *Handbook of LHC Higgs cross sections: 2. Differential distributions*, arXiv:1201.3084 [hep-ph].

[52] A. Bredenstein, A. Denner, S. Dittmaier and M. M. Weber, *Precise predictions for the Higgs-boson decay* $H \to WW/ZZ \to 4$ *leptons*, Phys. Rev. D **74** (2006) 013004 [hep-ph/0604011].

[53] A. Denner, S. Dittmaier, A. Muck, G. Passarino, M. Spira, C. Sturm, S. Uccirati and M. M. Weber, *Higgs production and decay with a fourth Standard-Model-like fermion generation*, Eur. Phys. J. C **72** (2012) 1992 [arXiv:1111.6395 [hep-ph]].

[54] S. Goria, G. Passarino and D. Rosco, *The Higgs boson lineshape*, arXiv:1112.5517 [hep-ph].

[55] S. Buehler, *Precise inclusive Higgs predictions using iHixs*, arXiv:1201.0985 [hep-ph].

[56] D. Berdine, N. Kauer and D. Rainwater, *Breakdown of the narrow-width approximation for New Physics*, Phys. Rev. Lett. **99** (2007) 111601 [hep-ph/0703058].

[57] N. Kauer, *Narrow-width approximation limitations*, Phys. Lett. B **649** (2007) 413 [hep-ph/0703077].

[58] N. Kauer, *A threshold-improved narrow-width approximation for BSM physics*, JHEP **0804** (2008) 055 [arXiv:0708.1161 [hep-ph]].

[59] C. F. Uhlemann and N. Kauer, *Narrow-width approximation accuracy*, Nucl. Phys. B **814** (2009) 195 [arXiv:0807.4112 [hep-ph]].

[60] E. W. N. Glover and J. J. van der Bij, *Vector boson pair production via gluon fusion*, Phys. Lett. B **219** (1989) 488.

[61] E. W. N. Glover and J. J. van der Bij, *Z-boson pair production via gluon fusion*, Nucl. Phys. B **321** (1989) 561.

[62] T. Binoth, M. Ciccolini, N. Kauer and M. Kramer, *Gluon-induced W-boson pair production at the LHC*, JHEP **0612** (2006) 046 [hep-ph/0611170].

[63] E. Accomando, *The process* $gg \to WW$ *as a probe into the EWSB mechanism*, Phys. Lett. B **661** (2008) 129 [arXiv:0709.1364 [hep-ph]].

[64] J. M. Campbell, R. K. Ellis and C. Williams, *Gluon-gluon contributions to W^+W^- production and Higgs interference effects*, JHEP **1110** (2011) 005 [arXiv:1107.5569 [hep-ph]].

[65] N. Kauer, *Signal-background interference in $gg \to H \to VV$*, arXiv:1201.1667 [hep-ph].

[66] L. J. Dixon and M. S. Siu, *Resonance-continuum interference in the diphoton Higgs signal at the LHC*, Phys. Rev. Lett. **90** (2003) 252001 [hep-ph/0302233].

[67] L. J. Dixon and Y. Sofianatos, *Resonance-continuum interference in light Higgs boson production at a photon collider*, Phys. Rev. D **79** (2009) 033002 [arXiv:0812.3712 [hep-ph]].

[68] E. Accomando, D. Becciolini, S. De Curtis, D. Dominici, L. Fedeli and C. Shepherd-Themistocleous, *Interference effects in heavy W'-boson searches at the LHC*, arXiv:1110.0713 [hep-ph].

[69] J. M. Campbell, R. K. Ellis and C. Williams, *Vector boson pair production at the LHC*, JHEP **1107** (2011) 018 [arXiv:1105.0020 [hep-ph]].

[70] R. Frederix, S. Frixione, V. Hirschi, F. Maltoni, R. Pittau and P. Torrielli, *Four-lepton production at hadron colliders: aMC@NLO predictions with theoretical uncertainties*, JHEP **1202** (2012) 099 [arXiv:1110.4738 [hep-ph]].

[71] T. Melia, K. Melnikov, R. Rontsch, M. Schulze and G. Zanderighi, *Gluon fusion contribution to W^+W^-+ jet production*, arXiv:1205.6987 [hep-ph].

[72] P. Agrawal and A. Shivaji, *Di-vector boson + jet production via gluon fusion at hadron colliders*, arXiv:1207.2927 [hep-ph].

[73] N. Kauer and D. Zeppenfeld, *Finite-width effects in top quark production at hadron colliders*, Phys. Rev. D **65** (2002) 014021 [hep-ph/0107181].

[74] G. Passarino, C. Sturm and S. Uccirati, *Higgs pseudo-observables, second Riemann sheet and all that*, Nucl. Phys. B **834** (2010) 77 [arXiv:1001.3360 [hep-ph]].

[75] S. Actis and G. Passarino, *Two-loop renormalization in the Standard Model, Part III: Renormalization equations and their solutions*, Nucl. Phys. B **777** (2007) 100 [hep-ph/0612124].

[76] A. Bredenstein, A. Denner, S. Dittmaier and M. M. Weber, *Precision calculations for $H \to WW/ZZ \to 4$ fermions with PROPHECY4f*, arXiv:0708.4123 [hep-ph].

[77] A. D. Martin, W. J. Stirling, R. S. Thorne and G. Watt, *Parton distributions for the LHC*, Eur. Phys. J. C **63** (2009) 189 [arXiv:0901.0002 [hep-ph]].

[78] D. de Florian (2012) private communication.

[79] D. Rebuzzi (2012) private communication.

[80] https://twiki.cern.ch/twiki/bin/view/LHCPhysics/VBF

[81] https://twiki.cern.ch/twiki/bin/view/LHCPhysics/WW

[82] https://twiki.cern.ch/twiki/bin/view/LHCPhysics/ZZ

[83] http://gg2VV.hepforge.org/

[84] T. Binoth, M. Ciccolini, N. Kauer and M. Kramer, *Gluon-induced WW background to Higgs boson searches at the LHC*, JHEP **0503** (2005) 065 [hep-ph/0503094].

[85] T. Binoth, N. Kauer and P. Mertsch, *Gluon-induced QCD corrections to $pp \to ZZ \to \ell\bar{\ell}\ell'\bar{\ell}'$*, arXiv:0807.0024 [hep-ph].

[86] T. Hahn and M. Perez-Victoria, *Automatized one-loop calculations in four and D dimensions*, Comput. Phys. Commun. **118** (1999) 153 [arXiv:hep-ph/9807565].

[87] T. Hahn, *Generating Feynman diagrams and amplitudes with FeynArts 3*, Comput. Phys. Commun. **140** (2001) 418 [arXiv:hep-ph/0012260].

[88] A. Djouadi, J. Kalinowski and M. Spira, *HDECAY: a program for Higgs boson decays in the Standard Model and its supersymmetric extension*, Comput. Phys. Commun. **108** (1998) 56 [hep-ph/9704448].

[89] G. Aad *et al.* [ATLAS Collaboration], *Search for the Standard Model Higgs boson in the decay channel* $H \to ZZ^* \to 4\ell$ *with* $4.8 fb^{-1}$ *of pp collision data at* $\sqrt{s} = 7$ *TeV with ATLAS*, Phys. Lett. B **710** (2012) 383 [arXiv:1202.1415 [hep-ex]].

[90] S. Chatrchyan *et al.* [CMS Collaboration], *Search for the Standard Model Higgs boson in the decay channel* $H \to ZZ \to 4$ *leptons in pp collisions at* $\sqrt{s} = 7$ *TeV*, Phys. Rev. Lett. **108** (2012) 111804 [arXiv:1202.1997 [hep-ex]].

[91] G. Aad *et al.* [ATLAS Collaboration], *Search for the Standard Model Higgs boson in the* $H \to WW^* \to \ell\nu\ell\nu$ *decay mode with* $4.7 fb^{-1}$ *of ATLAS data at* $\sqrt{s} = 7$ *TeV*, arXiv:1206.0756 [hep-ex].

[92] S. Chatrchyan *et al.* [CMS Collaboration], *Search for the Standard Model Higgs boson decaying to a W pair in the fully leptonic final state in pp collisions at* $\sqrt{s} = 7$ *TeV*, Phys. Lett. B **710** (2012) 91 [arXiv:1202.1489 [hep-ex]].

[93] A. J. Barr, B. Gripaios and C. G. Lester, *Measuring the Higgs boson mass in dileptonic W-boson decays at hadron colliders*, JHEP **0907** (2009) 072 [arXiv:0902.4864 [hep-ph]].

[94] G. Aad *et al.* [ATLAS Collaboration], *Search for a Standard Model Higgs boson in the* $H \to ZZ \to \ell\ell\nu\nu$ *decay channel using* $4.7\ fb^{-1}$ *of* $\sqrt{s} = 7$ *TeV data with the ATLAS detector*, arXiv:1205.6744 [hep-ex].

[95] S. Chatrchyan *et al.* [CMS Collaboration], *Search for the Standard Model Higgs boson in the* $H \to ZZ \to 2\ell 2\nu$ *channel in pp collisions at* $\sqrt{s} = 7$ *TeV*, JHEP **1203** (2012) 040 [arXiv:1202.3478 [hep-ex]].

[96] D. L. Rainwater and D. Zeppenfeld, *Observing* $H \to W^*W^* \to e^{\pm}\mu^{\mp}\not{p}_T$ *in weak boson fusion with dual forward jet tagging at the CERN LHC*, Phys. Rev. D **60** (1999) 113004 [Erratum-ibid. D **61** (2000) 099901] [hep-ph/9906218].